

# Scavenging of Radicals from the Gas Phase by Freezing with Dimethyl Disulfide

## 1. Test of the Method for Light Radicals

M. Schottler and K. H. Homann

Institut für Physikalische Chemie der Technischen Hochschule Darmstadt, Petersenstraße 20, D-6100 Darmstadt

*Elementary Reactions / Methods and Systems / Molecular Beams / Radicals*

H and O atoms and methyl radicals produced in microwave discharges of  $\text{H}_2/\text{He}$ ,  $\text{O}_2/\text{He}$  and  $\text{CH}_4/\text{He}$  mixtures, respectively, were scavenged by supersonic nozzle probing with subsequent freezing and reaction with dimethyl disulfide on a liquid nitrogen cooled wall. The main reaction products for the three kinds of radicals were  $\text{CH}_3\text{SH}$ ,  $\text{CH}_3\text{S(O)SCH}_3$  and  $\text{CH}_3\text{SCH}_3$ , respectively. Side products were  $\text{CH}_3\text{SCH}_2\text{SSCH}_3$  and  $\text{CH}_3\text{SSSCH}_3$  for H atoms and  $\text{CH}_3\text{S(O)}_2\text{SCH}_3$  for O atoms. — The scavenging efficiencies for the different radicals were determined and measured as a function of the gas phase radical concentration, the flow of scavenger molecules, the pressure in the vacuum chamber, and the conditions of the discharge and the flow through the sampling nozzle. It is concluded that this method is suitable for light radicals with reservations in the case of H atoms and can probably be used with still better success for heavier radicals.

### 1. Introduction

The identification and monitoring of radicals in the gas phase applying more commonly used methods such as (laser) optical methods, mass spectrometry and electron spin resonance is problematic in the case of larger hydrocarbon radicals. Radical scavenging has rarely been used in the gas phase [1] but is a well established method in the liquid phase [2].

We therefore combined molecular beam gas phase probing with radical scavenging in the condensed phase. The radicals in the molecular beam were frozen together with the scavenger molecules, dimethyl disulfide (DMD:  $\text{CH}_3\text{SSCH}_3$ ). Univalent radicals cleave the S-S bond [3], leading to a methyl sulfide and a methylthiyl radical as products. The latter radicals are unreactive and recombine [3–7]. The methyl sulfides can be separated and identified by gas chromatography/mass spectrometry (GC/MS).

In this paper we report on the method and its application to light radicals such as H and O atoms and methyl radicals.

### 2. Experimental

#### 2.1. Sample Production

The apparatus shown in Fig. 1 consisted essentially of three parts: a discharge flow system where the radicals could be produced, a conical nozzle beam probe and a liquid  $\text{N}_2$ -cooled plate in a high vacuum chamber. The radicals and the condensable beam particles were frozen there together with the dimethyl disulfide (DMD).

H and O atoms and methyl radicals were produced using a 2.45 GHz microwave discharge in  $\text{H}_2$ -He,  $\text{O}_2$ -He or  $\text{CH}_4$ -He, respectively, at pressures between 100 and 700 Pa. The discharge could be located either in a side tube ((a) in Fig. 1) or a few millimeters above the nozzle (b). The latter configuration was necessary for investigation of hydrocarbon radicals which disappear by rapid wall- and homogeneous reactions [8]. Some photolysis of DMD could not be avoided in this configuration (cf. 3.3). The concentrations of the gases in the flow tube were set and measured by capillary flow meters and low-pressure manostats [9] and by measuring the flow tube pressure.

The conical probe was made of quartz (height: 57 mm, apex angle:  $60^\circ$ ). Since it was also intended to apply this method to flames this probe is similar to the ones used previously on low-pressure flames [10]. The helium flow through the nozzle as a function of flow tube pressure was calibrated by measuring the pressure in the flow tube when it was only fed by the calibration leak and only pumped through the nozzle. This calibration was cross-checked by leading the helium from the calibration leak directly into the high vacuum chamber and measuring the resulting pressure.

Two orifice diameters,  $d$ , were used, 0.25 and 0.80 mm. The smaller hole was chosen when additional argon was admitted to the high-vacuum chamber to study the effects of scattering of the beam particles. Discharges in methane were studied using the larger hole to prevent clogging with polymeric material. The liquid  $\text{N}_2$ -cooled quartz plate (diameter 35 mm) was mounted in the centreline of the jet at a distance,  $\delta$ , of 10 cm from the nozzle tip. A jet of DMD was admitted through a copper tube equipped with a 0.5 mm nozzle (see Fig. 1). The flow of DMD vapour was controlled by a needle valve and was supplied from the gas phase above the liquid DMD stored at  $0^\circ\text{C}$ .

In order to get enough material for several analyses the collecting time was about 1 hour. After warm-up to room temperature under nitrogen whereby DMD melted ( $T_{\text{fus}} = -80^\circ\text{C}$ ) the sample was weighed and filled in vials of dark glass. The analyses were started immediately after sampling.

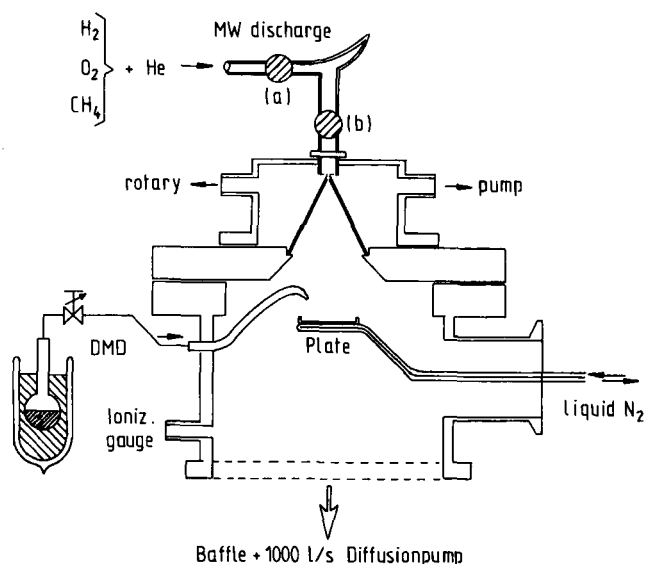


Fig. 1

Apparatus for scavenging of radicals by freezing together with dimethyl disulfide (DMD)

## 2.2. Analyses

The gas chromatograph (GC) was a dual column type (Varian 2740) modified by us for operation with capillary columns. Split injection onto capillary columns of different polarity was applied for an overall analysis and for the quantitative determination of the components with a mole fraction larger than 0.1%. A pre-column was used according to Deans [11] in order to detect trace components and to remove the excess DMD before using the capillary GC (column switching technique). This technique allowed to choose certain fractions from the pre-column for further capillary GC. Such a fraction was condensed in the first few centimeters of the capillary column by dry ice cooling. The capillary GC analysis was then started by rapid warm-up of the trap. Dry ice trapping worked effectively for substances with normal boiling points higher than about 80°C. Split injection had to be used to analyze more volatile substances. This method, however, was less sensitive by two orders of magnitude.

A flame ionization detector and a mass spectrometer, MS (Finnigan CH5), were used for quantitative analysis and identification, respectively. In the latter case an open split all-glas interface served as a connection between the GC and the MS.

## 2.3. Substances and GC Columns

Dimethyl disulfide (DMD, Merck) was always freshly distilled under argon and had better than 99.5% purity. Impurities were benzene, triethyl amine, methyl-*t*-butyl sulfide and a hydrocarbon C<sub>8</sub>H<sub>16</sub>.

Gases were supplied by Messer-Griesheim: He (99.996 and 99.999%), Ar (99.997%), H<sub>2</sub> (99.999%), O<sub>2</sub> (99.995%) and by Linde: CH<sub>4</sub> (99.95%) and were used without further purification for the discharges. The GC carrier gas (He) was further purified by an Oxisorb cartridge (Messer-Griesheim).

Columns used with the split injection were a) 15 m × 0.5 mm i.d. Squalan SCOT steel column, b) 25 m × 0.32 mm i.d. OV1701 (chem. bond.) fused silica column, 0.25 μm film thickness. Coupled columns: 1.8 m × 2 mm i.d. glass column packed with 3% OV17 on Chromosorb 80/100 mesh together with a 50 m × 0.32 mm i.d. SE30 (chem. bond.) fused silica capillary, 0.25 μm film thickness.

## 3. Results

### 3.1. Products from the Scavenging Reactions

#### Blank Runs

The only detectable compound formed when helium (99.9996%) streamed through the discharge was 2,3,5-trithiahexane (TTH: CH<sub>3</sub>SSCH<sub>2</sub>SCH<sub>3</sub>). It is a known photolysis product of DMD [12]. It was always formed in a fraction of about 5 · 10<sup>-5</sup> independent of the nozzle flow when the discharge was directly above the probe and UV light fell on the plate.

When using the 99.996% helium in the discharge, methanethiosulfonic acid *S*-methyl ester (TSI) was also detectable in trace amounts. It resulted from oxygen impurities in the helium (see below).

#### H Atoms

Methanethiol (MTL: CH<sub>3</sub>SH) is the main product of the reaction. Two minor products dimethyl trisulfide (DMT: CH<sub>3</sub>SSSCH<sub>3</sub>) and 2,3,5-trithiahexane (TTH), both in an amount of 10<sup>-2</sup> to 10<sup>-3</sup> relative to MTL, resulted also from the scavenging process. The three components were identified by comparing their respective mass spectra to reference spectra [13,14]. Because of its low boiling point, losses of MTL occurred in the process of sample handling.

#### O Atoms

O atoms yield methanethiosulfonic acid-*S*-methyl ester (TSI) and minor amounts of methanethiosulfonic acid *S*-methyl ester (TSO) together with traces of DMT and TTH.



TSI and TSO were identified by their respective mass spectra (TSI: [15], TSO: authentic sample (Aldrich Chemie)).

Moreover, the Kovats index [16] of TSO on SE30 was identical to that of a reference sample.

#### Methyl Radicals

Dimethyl sulfide (DMS: CH<sub>3</sub>SCH<sub>3</sub>) and methanethiol (MTL) were the only major products from radicals out of the CH<sub>4</sub> discharge. DMS was identified by its mass spectrum [13]. The concentrations of DMS and MTL in the sample were comparable. This means, however, that in the flow tube H atoms were much more abundant than CH<sub>3</sub> radicals since the scavenging efficiency of H is much lower than that of CH<sub>3</sub> (cf. 3.6, 4.2).

No other products from a reaction with methyl radicals could be detected. Besides MTL, DMT and TTH which are due to the reaction with H atoms, we detected trace amounts of ethyl methyl disulfide and 2,4-dithiapentane, which both might be scavenging products from CH<sub>2</sub>. The concentrations of these two compounds were usually less than 0.1% of the DMS concentrations in the sample.

### 3.2. Definition of a Scavenging Efficiency

In order to have a measure of the amount of scavenging products obtained from a certain concentration of a specified radical or atom in the flow tube, a scavenging efficiency  $A(i,j)$  of a radical (or atom)  $i$  forming a sulfur containing product  $j$  is defined:

$$A(i,j) \stackrel{\text{def}}{=} \frac{\dot{N}_r(i,j)}{\dot{N}_0(i) \cdot \nu_{ij}}$$

$\dot{N}_r(i,j)$  is the number per time of product molecules  $j$  formed on the plate from the radical  $i$ .  $\dot{N}_0(i)$  is the number per time of radicals  $i$  flowing through the nozzle. It is proportional to their concentration in the flow tube.  $\nu_{ij}$  is a stoichiometric coefficient of product  $j$  in the overall scavenging reaction of radical  $i$ . It is normally equal to one.  $\dot{N}_r(i,j)$  is obtained from the quantitative GC analysis, the total mass of the liquid sample and the sampling time. The number flow of radicals through the nozzle could only be estimated from the degree of dissociation  $\alpha$  of the respective molecules by the discharge as found in previous experiments under the same conditions or in the literature ( $\alpha \approx 0.3$  for O<sub>2</sub> and H<sub>2</sub> [9]). The fraction of CH<sub>3</sub> generated from CH<sub>4</sub> is approximately 0.02 [17].  $A(i,j)$  is always less than unity and depends on factors discussed below.

Trithiahexane (TTH) is an example for an unspecific scavenging product since it may be formed from many different radicals (see 4.1). Although scavenging efficiencies  $A(i, \text{TTH})$  may be defined and measured it is not useful to monitor TTH formation from the reaction of a mixture of radicals with DMD.

A somewhat similar case is the product TSO. Its formation from O atoms is obviously positively influenced by the presence of O<sub>2</sub> (see 3.3 and 4.1). Therefore a scavenging efficiency of O with respect to TSO is not given and the number formation rate is denoted only by  $\dot{N}_r(\text{TSO})$ . In the present investigation difficulties of this kind arise only in the analysis of side products.

### 3.3. Variations of O and H Concentrations

Under the conditions of Fig. 2 there is a linear relationship between  $\dot{N}_r(\text{O, TSI})$  and  $\dot{N}_0(\text{O})$  up to at least  $\dot{N}_0(\text{O}) = 6 \cdot 10^{15} \text{ s}^{-1}$  corresponding to an  $A(\text{O, TSI}) \approx 0.05$ . Above this O atom flow there starts a deviation from linearity to lower scavenging efficiency. During these measurements the flow of DMD was held constant. It can be characterized by the number per time of DMD molecules condensing on the cold plate,  $\dot{N}_c(\text{DMD})$ , which was  $5.0 \cdot 10^{16} \text{ s}^{-1}$ . Since it is not possible to determine an equivalence ratio of DMD molecules to atoms (or radicals) impinging on the plate the ratio  $Y(i) \stackrel{\text{def}}{=} \dot{N}_c(\text{DMD})/\dot{N}_0(i)$  was used as a parameter to compare scavenging efficiencies for different radicals  $i$  at different condensing rates of DMD. An  $\dot{N}_0(\text{O})$  corresponding to  $Y(\text{O}) = 5$  is indicated on Fig. 2: increasing  $\dot{N}_0(\text{O})$  signifies decreasing  $Y(\text{O})$ . In terms of

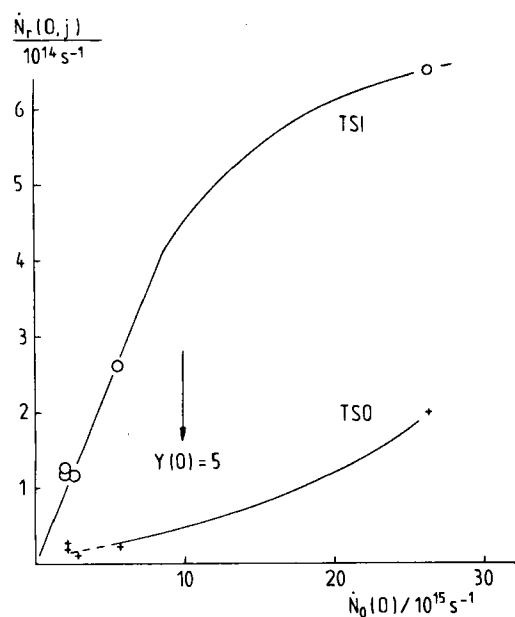


Fig. 2

Influence of the inflow of oxygen atoms through the nozzle ( $\dot{N}_0(O)$ ) on the number rate of formation of products; TSI:  $\text{CH}_3\text{S(O)SCH}_3$ , TSO:  $\text{CH}_3\text{S(O)}_2\text{SCH}_3$ , condensing scavenger flow  $\dot{N}_c(\text{DMD}) = 5 \cdot 10^{16} \text{ s}^{-1}$ , background pressure  $p_\infty(\text{Ar}) = 0.026 \text{ Pa}$ ,  $\lambda_\infty/\delta = 3.8$ ,  $Kn_0^{-1} = 3.2$ ,  $d = 0.25 \text{ mm}$ ; the symbols not explained here are explained in the text

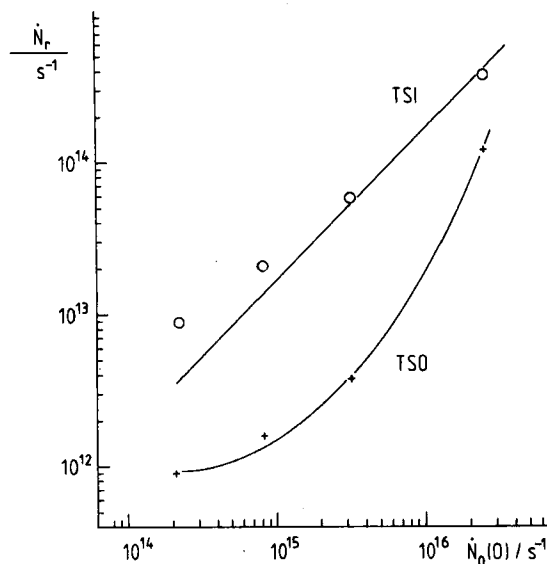


Fig. 3

Extension of the measurement of products to low oxygen atom inflow;  $\dot{N}_c(\text{DMD}) = 2 \cdot 10^{17} \text{ s}^{-1}$ ,  $Kn_0^{-1} = 7.4$ ,  $p_\infty(\text{He}) = 0.30 \text{ Pa}$ ,  $d = 0.80 \text{ mm}$ ,  $\lambda_\infty/\delta = 0.44$

$Y(O)$  there is noticeable decrease in  $A(O, \text{TSI})$  at values lower than about 5. The decrease of  $Y(O)$  which means a smaller surplus of DMD at the plate is held to be responsible for the decrease of  $A(O, \text{TSI})$  (cf. Fig. 3).

In the linear range of TSI formation the rate,  $\dot{N}_r(\text{TSO})$ , is only about 8% of the TSI formation rate. When  $\dot{N}_0(O)$  is increased, i.e.  $Y(O)$  is decreased, a more than proportional increase of TSO formation rate sets in, raising the relative TSO yield to about 25% of the scavenging products.

The total pressure in the high vacuum chamber at the conditions of Fig. 2, being mainly due to the added background gas argon, was comparatively low (cf. legend).

The lower part of the linear range for TSI formation was also investigated using the more sensitive column switching GC method. The results shown in a logarithmic diagram in Fig. 3 were obtained under somewhat different conditions of pressure and DMD flow (see legend). The straight line has a slope of unity and has been fitted to the upper two points. It corresponds to  $A(O, \text{TSI}) = 0.016$ . This lower scavenging efficiency is caused by more scattering of the O atoms due to the higher background pressure as a consequence of the larger nozzle diameter. On the other hand is the linear range extended to an O atom flow of at least  $2.5 \cdot 10^{16} \text{ s}^{-1}$ . This is due to the also increased condensation rate of DMD which corresponds to  $Y(O) = 8.0$  at this  $\dot{N}_0(O)$ .

At very low flows of O atoms there is an apparent departure from linearity between  $\dot{N}_r(O, \text{TSI})$  and the nominal  $\dot{N}_0(O)$  to higher values of  $\dot{N}_r(O, \text{TSI})$ . This, however, is due to an oxygen impurity in the helium raising the  $\dot{N}_0(O)$  above the nominal value fixed by the flow control of oxygen and the discharge power. In a blank run using the same helium tank TSI was detected at a rate of  $\dot{N}_r(O, \text{TSI}) = 2 \cdot 10^{12} \text{ s}^{-1}$ . Taking the scavenging efficiency for larger O atom flow and a degree of  $\text{O}_2$  dissociation of  $\approx 0.3$  a volume ratio of oxygen in the helium of  $2 \cdot 10^{-5}$  was obtained. The sum of impurities stated by the supplier was  $4 \cdot 10^{-5}$ .

For methanethiol (MTL), the main scavenging product from H atoms, only semi-quantitative results could be obtained which were not free from scatter, due to evaporation losses during preparation for analysis. The scavenging efficiencies,  $A(\text{H}, \text{MTL})$  for different H atom flows were of the order of  $1 \cdot 10^{-3}$ . Therefore experimental results with varying H atom flow are reported only for 2,3,5-trithiahexane (TTH) which was a side product but could be analyzed with much better reproducibility.

Fig. 4 shows the production of TTH as a function of the H atom flow for the conditions given in the legend. At zero and low  $\dot{N}_0(\text{H})$  TTH is mainly produced in this experiment by photolysis through UV-light from the discharge. For larger H atom flow there is a region of almost constant scavenging efficiency,  $A(\text{H}, \text{TTH}) = 1.8 \cdot 10^{-5}$ . Since the nozzle flow of H atoms was much larger than that of O atoms in Figs. 2, 3 it is interesting to note that the region of constant  $A(\text{H}, \text{TTH})$  extends into a range of  $Y(\text{H}) < 1$ , whereas  $A(O, \text{TSI})$  begins to decrease when  $Y(O) \lesssim 5$ . An explanation for this different behaviour may be the stronger scattering of H atoms.

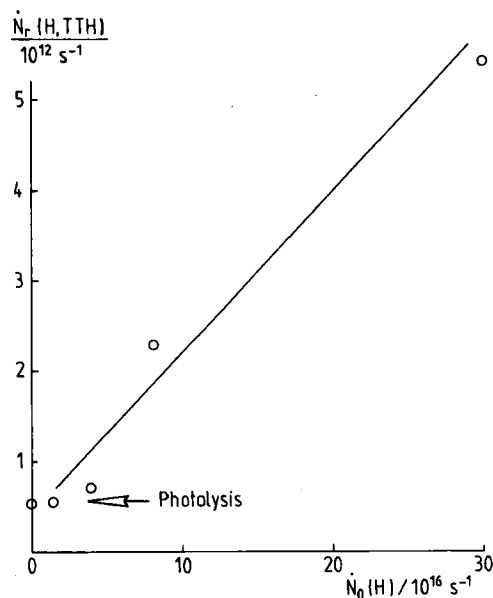


Fig. 4

Number rate of 2,3,5-trithiahexane formation by hydrogen atoms as a function of hydrogen atom inflow through the nozzle;  $\dot{N}_c(\text{DMD}) = 1.3 \cdot 10^{17} \text{ s}^{-1}$ ,  $p_\infty(\text{He}) = 0.20 \text{ Pa}$ ,  $\lambda_\infty/\delta = 0.9$ ,  $Kn_0^{-1} = 13$ ,  $d = 0.80 \text{ mm}$

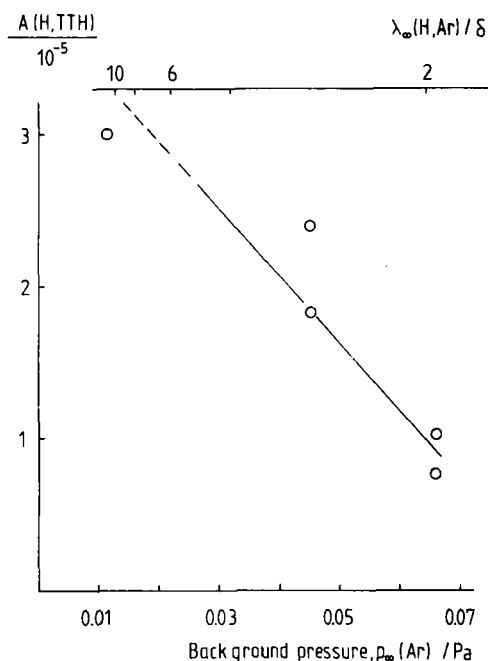


Fig. 5

Influence of scattering (background gas pressure) on the scavenging efficiency of hydrogen atoms,  $A(\text{H, TTH})$ ;  $\dot{N}_c(\text{DMD}) = 5 \cdot 10^{16} \text{ s}^{-1}$ ,  $Kn_0^{-1} = 6.3$ ,  $d = 0.25 \text{ mm}$ ,  $\dot{N}_0(\text{H}) = 1 \cdot 10^{17} \text{ s}^{-1}$

### 3.4. Variation of the High-Vacuum Pressure

The pressure in the high vacuum chamber was varied in order to investigate the influence of scattering on the scavenging of radicals. This influence should be most noticeable in the case of H atoms. TTH was monitored as the product.

In one experiment argon was admitted as a background gas to the chamber. Fig. 5 shows how  $A(\text{H, TTH})$  decreases when the background pressure  $p_\infty(\text{Ar})$  is increased.  $A(\text{H, MTL})$  values showed a similar behaviour but were much less reproducible (cf. 3.3). The upper abscissa is scaled by  $\lambda_\infty(\text{H, Ar})/\delta$ , the ratio of the

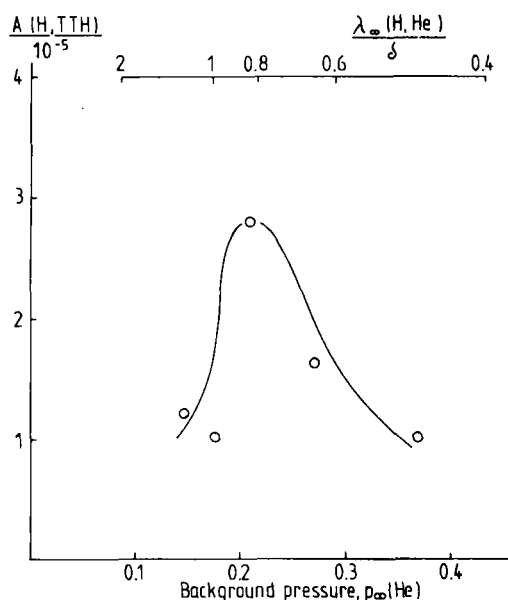


Fig. 6

Variation of background gas pressure by variation of total nozzle flow,  $\dot{N}_0(\text{He})$ ;  $\dot{N}_c(\text{DMD}) = 1.6 \cdot 10^{17} \text{ s}^{-1}$ ,  $d = 0.80 \text{ mm}$ ,  $\dot{N}_0(\text{H}) = 9 \cdot 10^{16} \text{ s}^{-1}$

mean free path (with respect to H–Ar collisions) to the distance between the nozzle and the plate.  $\lambda_\infty(\text{H, Ar})$  was calculated using the formulae for thermally equilibrated flow, since it does not depend very much on the difference of the mean beam velocity of H atoms to their average thermal velocity at room temperature. The collision diameters were taken from [18] for H and O atoms for Ar and for He.

When no additional Ar was admitted and instead the pressure in the vacuum chamber raised by increasing the helium pressure in the flow tube,  $A(\text{H, TTH})$  passed through a maximum at  $\lambda_\infty(\text{H, He})/\delta \approx 1$ , as shown in Fig. 6. First  $A(\text{H, TTH})$  increases because of an increase in the inverse source Knudsen number of the nozzle flow which causes a narrowing of the beam. At a further raise of pressure beam scattering outweighs this effect and the scavenging efficiency decreases.

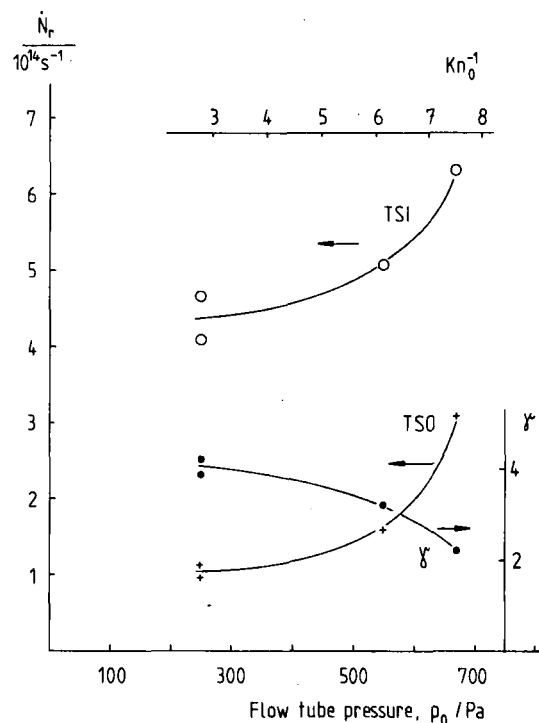


Fig. 7

Influence of the flow tube pressure on the number rate of formation of scavenging products at constant oxygen atom inflow;  $\dot{N}_c(\text{DMD}) = 5 \cdot 10^{16} \text{ s}^{-1}$ ,  $\dot{N}_0(\text{O}) = 2.9 \cdot 10^{16} \text{ s}^{-1}$ ,  $p_\infty(\text{Ar}) = 0.026 \text{ Pa}$ ,  $\lambda_\infty/\delta = 3.8$ ,  $d = 0.25 \text{ mm}$

### 3.5. Variation of the Inverse Source Knudsen Number

The inverse source Knudsen number  $Kn_0^{-1} \stackrel{\text{def}}{=} d/\lambda_0(\text{He})$  is a parameter for describing the transition from effusion ( $Kn_0^{-1} \ll 1$ ) to continuum flow ( $Kn_0^{-1} \gg 1$ ). Here  $d$  is the nozzle diameter and  $\lambda_0(\text{He})$  is the mean free path of helium at stagnation conditions in front of the nozzle.  $Kn_0^{-1}$  is proportional to the flow tube pressure  $p_0$  ( $\approx p_0(\text{He})$ ).

In the experiment with O atoms  $p_0(\text{He})$  was varied while keeping the background pressure in the vacuum chamber, mainly  $p_\infty(\text{Ar})$ , at 0.026 Pa by adding more or less argon. This corresponds to a ratio  $\lambda_\infty(\text{O, Ar})/\delta = 3.8$  implying a low degree of scattering in the free molecular flow regime. The flow of O atoms through the nozzle,  $\dot{N}_0(\text{O})$ , was held approximately constant during the variation of  $p_0$ . Fig. 7 shows that an increase of  $Kn_0^{-1}$  increases the formation rate of both TSI and TSO.  $\dot{N}_r(\text{TSO})$  increases more rapidly than  $\dot{N}_r(\text{O, TSI})$  as shown by the fall-off of the ratio  $\gamma = \dot{N}_r(\text{O, TSI})/\dot{N}_r(\text{TSO})$ .

As in the case of H atoms a narrowing of the beam increased the O atom flow onto the plate causing a larger product formation rate and thereby a larger scavenging efficiency. An increase of the O atom flow onto the plate, no matter whether it was effected by increasing the O atom concentration in the flow tube (cf. 3.3) or by

narrowing the beam, led to a relatively stronger increase in TSO than in TSI formation.

### 3.6. Variation of the Microwave Power in CH<sub>4</sub>-Discharges

MW discharges in hydrocarbons can lead to the formation of many different radical intermediates through primary and secondary reactions. Their absolute and relative concentrations depend on the mw power, all other conditions remaining constant [8]. The influence on the formation of H atoms and methyl radicals in a methane/helium discharge is shown in the following table:

Table 1  
DMS and MTL from methane/helium discharges

Nominal microwave power	30 W	50 W
Residence time	0.1 ms	0.1 ms
$p_0$	350 Pa	350 Pa
$Y(\text{CH}_3)$	> 500	> 500
$\dot{N}_r(\text{CH}_3, \text{DMS})/\text{s}^{-1}$	$1.3 \cdot 10^{14}$	$5.6 \cdot 10^{13}$
$\dot{N}_r(\text{H, MTL})/\text{s}^{-1}$	$1.5 \cdot 10^{14}$	$2.5 \cdot 10^{14}$

Without the discharge  $\dot{N}_0(\text{CH}_4)$  was  $4.7 \cdot 10^{16} \text{ s}^{-1}$ . If a degree of dissociation to CH<sub>3</sub> of 2% at 30 W is assumed [17],  $A(\text{CH}_3, \text{DMS})$  is equal to 0.14. Since the concentration of CH<sub>3</sub> was not known exactly this is only an approximate value which, however, is of the same order as that of  $A(\text{O, TSI})$ , while that of  $A(\text{H, MTL})$  is distinctly smaller ( $\approx 1 \cdot 10^{-3}$ ).

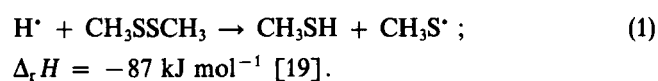
The fact that  $\dot{N}_r(\text{CH}_3, \text{DMS})$  and  $\dot{N}_r(\text{H, MTL})$  were comparable at 30 W mw power signified that much more H atoms than methyl radicals were formed in the discharge, the ratio being of the order of 10<sup>2</sup>. With increasing mw power more H atoms but less CH<sub>3</sub> radicals were formed so that this ratio increased further.

## 4. Discussion

### 4.1. Mechanisms of the Scavenging Reactions

#### H Atoms

The main product of the reaction, CH<sub>3</sub>SH, is formed by the displacement reaction



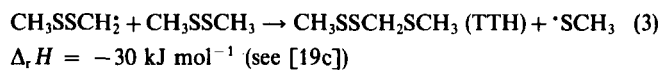
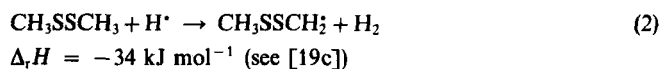
This reaction has a rate constant of  $5 \cdot 10^{12} \text{ cm}^3 \text{ mol}^{-1} \text{ s}^{-1}$  in the gas phase at room temperature and its activation energy has been found to be almost zero [4]. This would be in line with a rapid reaction also in a matrix at 77 K for which Symons et al. found evidence when studying the effect of added DMD on the radiolysis products of thiols [5].

That the scavenging efficiency in our apparatus is nevertheless comparatively low is due to the scattering of H atoms and probably to an appreciable reflection at the plate.

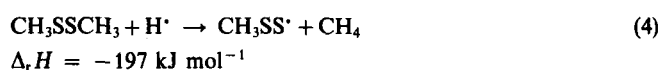
Evidence for the presence of radicals in the matrix was obtained by inspection of the cold sample. When removed from the chamber under nitrogen the cold matrix showed a yellow colour which disappeared on warming. This was also found when scavenging O atoms. A similar observation was made by Chang et al. [7] who froze the products of a reaction of CH<sub>3</sub>SH with radicals (H, OH, O etc.) from a discharge in water vapour. They report the disappearance of a pink colour and even occasional explosions when warming up the cold trap. In our reaction, H + DMD, the colour may

be ascribed to thiyl radicals (CH<sub>3</sub>S) which recombine on warming. A reaction of CH<sub>3</sub>S with H atoms seems not important since H is rapidly consumed by the excess DMD.

The formation of the minor products, TTH and DMT, may be explained by two reaction sequences initiated by C–H and C–S bond breaking, respectively:



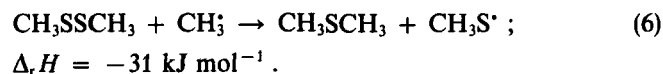
and



It is most likely that the abstracting radical is the H atom and not the thiyl radical since the latter has to be electronically excited to abstract an H atom from the methyl group of a disulfide [6]. Other radicals, however, can also react in analogy to reactions (2) and (4) so that TTH and DMT are not products specific for H atom scavenging.

#### Methyl Radicals

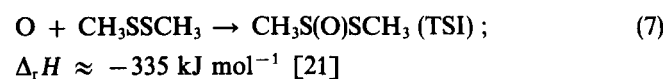
The scavenging product results from the cleavage of the S–S bond as in the case of H atoms:



Reaction (6) is at least 6 orders of magnitude slower in the gas phase than reaction (1) [20]. We estimate, however, a fraction of 14% of the inflowing methyl radicals to react on the plate. This indicates that the order of magnitude of the rate constant in the gas phase does not influence the fraction of scavenged radicals.

#### O Atoms

Judging from the nature of the products, addition rather than displacement reactions prevail in the scavenging of O atoms. There is evidence that in the gas phase the addition reaction

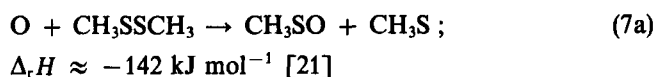


leads to decomposition and further reaction of intermediates [21]. However, in the matrix this simple step certainly plays a major role leading directly to the main scavenging product. An equally simple consecutive reaction



can lead to the side product, explaining the nearly quadratic dependence of the TSO formation rate on  $\dot{N}_0(\text{O})$  at relatively

high O atom flow (cf. 3.3). But we have evidence that there are other sources of TSO, at least at low O atom flow where an almost constant fraction of TSO seems to accompany the TSI formation. Furthermore, we found a positive influence of molecular oxygen on TSO formation which is most noticeable at low O atom flow while TSI is not influenced. A tentative explanation is given as follows: Despite the contact to condensed DMD the addition of O to DMD leads to a rupture of the S–S bond via a minor channel of reaction (7):



(Remember the vanishing colour of the matrix!).

An immediate recombination of the primary  $\text{CH}_3\text{SO}$  and  $\text{CH}_3\text{S}$  in their matrix cage may be hindered by "chemical diffusion" [22] of the thiyl radicals via a reaction



which would be supported by a local heating of the matrix through reaction (7a). The radicals formed in (7a) can then recombine in three combinations during warm-up



Reaction (11) may yield a constant fraction of TSO relative to TSI since varying  $\dot{N}_0(\text{O})$  which leads to varying thiyl- and sulfanyl radical concentrations in the matrix does not influence the relative rates of reactions (10), (11) and (12). This is valid as long as (7a) is the only source of thiyl- and sulfanyl radicals in the system.

Molecular oxygen may react with the intermediate sulfur-containing radicals opening several further possibilities for TSO formation [3]. An uncontrolled oxygen content in the high vacuum chamber may therefore be the reason for the scatter in the TSO data at low O atom flow (Fig. 2).

The decreasing scavenging efficiency with decreasing  $Y(i)$  is attributed to the recombination of radicals on the surface of the freezing DMD when their surface concentration becomes too large. The recombination products,  $\text{H}_2$ ,  $\text{O}_2$ ,  $\text{C}_2\text{H}_6$ , were not frozen in the matrix or evaporated during the warm-up, respectively, so that they would not be detected by this method. From the gas-phase reaction of  $\text{H} + \text{DMD}$ ,  $\text{O} + \text{DMD}$  and  $\text{CH}_3 + \text{DMD}$  it is known that no other volatile products are formed [4, 20, 21].

#### 4.2. Molecular Scattering

It is not only the chemical reactions of the radicals and their mechanisms that have a bearing on the scavenging efficiency of the different radicals but also the conditions of flow in the vacuum chamber and the interaction of the radical-containing gas beam with the plate and the background gas. Factors that influence the scavenging efficiency are geometric dimensions, such as the ratio of the plate area to the

"cross section" of the nozzle beam, scattering of the radicals and reflection from the plate. Since no direct measurements of gas dynamic properties of the beam have been made these influences can only be estimated.

There was a second beam, the scavenger beam, which in contrast to the nozzle beam contained only particles that would condense under equilibrium conditions at a plate temperature of 77 K. Actually only 25% of the total inflow of DMD condensed on the plate. Since the distance of the DMD inlet to the plate was such that more than 90% of the DMD molecules should have directly hit the plate the reflection factor was 75% or probably larger since a part of the DMD on the plate resulted from condensation of background DMD. Therefore it can be concluded that the fraction of the non-condensing radicals that is reflected from the plate is at least of the same order if not larger.

The theoretical treatment of the interaction of a rarefied supersonic flow with a plate is a difficult problem. It has been discussed by Kogan [25]. No shock in the continuum sense can exist in front of the plate but beam destruction due to molecular scattering may be important. Losses by scattering can have different causes. Scattering in the free molecular flow regime is mainly dependent on the pressure of the background gas and becomes important when  $\lambda_\infty/\delta \lesssim 1$ , particularly for light radicals. If it is assumed that every collision of an H atom with an Ar atom under the conditions of Fig. 5 prevents the H from reaching the plate then the decrease in TTH formation should be proportional to  $\exp(-\sigma(\text{H}, \text{Ar}) \cdot C(\text{Ar}) \cdot l)$  [26] where  $\sigma$  is the collision cross section,  $C$  the number density, and  $l$  the path length. There are not enough accurate data points in Fig. 5 to verify this dependence. Setting  $l$  equal to 0.1 m, the distance between the nozzle and the plate, a  $\sigma(\text{H}, \text{Ar}) \approx 8 \cdot 10^{-19} \text{ m}^2$  would result from the relative decrease of  $A(\text{H}, \text{TTH})$  per change in background pressure. This is high compared to the gas kinetic value of  $2.3 \cdot 10^{-19} \text{ m}^2$  for H–Ar collisions [18] and shows that other influences further weaken the beam of H atoms. It can be expected that O atoms and heavier radicals are not so much subject to being scattered completely out of the beam in the molecular flow regime if the background gas is mainly helium. Because of the larger mass ratio a collision does not deflect heavier particles in the same measure as it does affect H atoms.

An extrapolation of  $A(\text{H}, \text{TTH})$  and also of  $A(\text{H}, \text{MTL})$  (not shown) to zero background pressure leads to still much lower values than the scavenging efficiencies for O or  $\text{CH}_3$ . This shows that a great deal of H scattering takes place in the continuum flow regime of the expanding gas. The mass separation effect in the supersonic free jet of a gas mixture is such that the heavy components are relatively enriched in the beam axis while the light component is distributed over the entire beam cross section which in this case is limited by the geometry of the cone. This lateral expansion of the H atom flow leads to a small surface concentration of H on the plate. Accordingly the flow of DMD, i.e.  $Y(\text{H})$ , can be much lower than in the case of the heavier O atoms before the recombination of H on the plate comes into concurrence with the reaction with DMD.

Kogan [25] has discussed the scattering of beam particles by molecules that are directly reflected from the plate. This

is only discernible from background scattering when the number density of reflected molecules near the plate is larger than or comparable to the background number density. Molecules that are reflected from the plate in our experiments are mainly the scavenger molecules (DMD) and helium atoms:

- The flow of DMD molecules typically reflected from the plate be  $2 \cdot 10^{17} \text{ s}^{-1}$ . The molecules leave the surface across an area of the order of  $L^2 = 1.2 \cdot 10^{-3} \text{ m}^2$  ( $L =$  plate diameter  $= 3.5 \text{ cm}$ ) with a thermal (77 K) velocity of  $130 \text{ m s}^{-1}$ . This results in a number density of reflected DMD molecules in the vicinity of the plate of  $1.3 \cdot 10^{18} \text{ m}^{-3}$ .
- The helium atom flow through the 0.25 mm nozzle at a flow tube pressure of 500 Pa is  $1.2 \cdot 10^{18} \text{ s}^{-1}$ . If the reflected flow is about  $0.5 \cdot 10^{18} \text{ s}^{-1}$  with an average velocity of  $1200 \text{ m s}^{-1}$ , since He is little accommodated at the cold surface, a number density of  $3.5 \cdot 10^{17} \text{ m}^{-3}$  is obtained.

Both number density values are small compared to the background number density of argon,  $6.5 \cdot 10^{18} \text{ m}^{-3}$ , corresponding to  $p_{\infty}(\text{Ar}) = 0.026 \text{ Pa}$  so that the extra scattering effect due to reflected particles is also small.

#### 4.3. Gas Phase Reactions

The estimated number density of reflected DMD molecules in front of the plate may also be used to evaluate the percentage of radicals that undergo gas phase reactions with the DMD.

The fastest of the scavenging reactions investigated was the O + DMD reaction which at 300 K has a rate coefficient of  $6 \cdot 10^{13} \text{ cm}^3 \text{ mol}^{-1} \text{ s}^{-1}$  in the gas phase [27]. The scavenger molecules reflected from the plate have a number density of  $1.3 \cdot 10^{18} \text{ m}^{-3}$  which leads to a reaction probability of about 1% for O atoms passing the gas phase towards the plate. There may be an enhanced number density of scavenger molecules in the incoming beam of dimethyl disulfide. We estimate a number density of  $9 \cdot 10^{18} \text{ m}^{-3}$  at a characteristic radial extension of 1 cm of the beam. However, the reaction probability in the gas phase remains small since due to its small diameter the scavenger beam is crossed only by a part of the oxygen atoms.

#### 5. Conclusions

It has been shown that this scavenging method for radicals from a low-pressure gas phase can be used for the quantitative analysis of small radicals. The kind of scavenging reaction, addition or displacement, and its corresponding rate constant in the gas phase is of minor importance for the scavenging efficiency. For very light radicals such as H atoms the method is less suitable since large scattering and reflection effects cause a low scavenging efficiency and the low radical mass leads to very volatile products. The method should even be more useful for heavier radicals. A disadvantage is the comparatively long sampling and analysis time but this may well be compensated by the advantage that many different radicals can be identified and measured in one run.

The work was supported by the Deutsche Forschungsgemeinschaft and by the Fonds der Chemischen Industrie. This is gratefully acknowledged.

#### References

- [1] R. M. Fristrom, *Science* **140**, 297 (1963); J. V. Volponi, W. J. McLean, R. M. Fristrom, and Z. A. Muir, *Combust. Flame* **65**, 243 (1986).
- [2] T. Koenig and H. Fischer, in: *Free Radicals*, Vol. I, p. 163, ed. J. K. Kochi, John Wiley & Sons, New York 1973.
- [3] J. K. Kice, in: *Free Radicals*, Vol. II, p. 719, ed. J. K. Kochi, John Wiley & Sons, New York 1973.
- [4] M. M. Ekwenchi, A. Jodhan, and O. P. Strausz, *Int. J. Chem. Kinet.* **12**, 431 (1980).
- [5] R. L. Petersen, D. J. Nelson, and M. C. R. Symons, *J. Chem. Soc. Perk. Trans. II*, 1978, 225.
- [6] M. Ya. Mel'nikov and N. V. Fok, *Khim. Vys. Energ.* **10**, 466 (1976).
- [7] C. H. Chang, P. L. Goodfriend, M. D. Bentley, and R. J. Anderegg, *Can. J. Chem.* **61**, 1617 (1983).
- [8] K. H. Homann, W. Lange, and H. Gg. Wagner, *Ber. Bunsenges. Phys. Chem.* **75**, 121 (1971).
- [9] J. Grebe, Dissertation, Darmstadt (D17) 1981; J. Grebe and K. H. Homann, *Ber. Bunsenges. Phys. Chem.* **86**, 58 (1982).
- [10] K. H. Homann, M. Mochizuki, and H. Gg. Wagner, *Z. Phys. Chem. Neue Folge* **37**, 299 (1963).
- [11] D. R. Deans, *Chromatographia* **1**, 8 (1968).
- [12] R. G. Buttery and R. M. Seifert, *J. Agric. Food Chem.* **25**, 434 (1977).
- [13] E. Stenhagen, S. Abrahamsson, and F. W. McLafferty (eds.), *Atlas of Mass Spectral Data*, Vol. 1, Interscience Publishers 1969.
- [14] R. G. Buttery, D. G. Guadagni, L. C. Ling, R. M. Seifert, and W. Lipton, *J. Agric. Food Chem.* **24**, 829 (1976).
- [15] A. Kjaer, J. O. Madsen, A. Maeda, Y. Ozawa, and Y. Uda, *Agric. Biol. Chem.* **42**, 1715 (1978).
- [16] E. Kováts, *Helv. Chim. Acta* **41**, 1915 (1958).
- [17] N. N. Dogramadze and K. F. Zmbov, *Bull. Inst. Nucl. Sci. Boris Kidrich* **9**, 6188 (1958), cited according to F. P. Lossing, in: *Mass Spectrometry*, ed. C. A. McDowell, p. 484, McGraw Hill, New York 1963.
- [18] J. Warnatz, *Habilitationschrift*, Darmstadt (D17) 1977.
- [19]  $\Delta_f H^0$  values for radicals and stable compounds were taken from: a) D. L. Baulch, R. A. Cox, R. F. Hampson, jr., J. A. Kerr, J. Troe, and R. T. Watson, *J. Phys. Chem. Ref. Data* **9**, 295 (1980) (for H, O, CH<sub>4</sub>); b) S. P. Heneghan, P. A. Knoot, and S. W. Benson, *Int. J. Chem. Kinet.* **13**, 677 (1981) (for CH<sub>3</sub>); c) L. G. S. Shum and S. W. Benson, *Int. J. Chem. Kinet.* **15**, 433 (1983) (for CH<sub>3</sub>S); d) S. W. Benson, *Chem. Rev.* **78**, 23 (1978) (for CH<sub>3</sub>SS); e) D. D. Wagman, W. H. Evans, U. B. Parker, I. Halow, S. M. Bailey, and R. H. Schumm, *N.B.S. Tech. Note* 270-3, Government Printing Office, Washington, D.C. 20402 (1968) (for CH<sub>3</sub>SH, CH<sub>3</sub>SCH<sub>3</sub>, CH<sub>3</sub>SSCH<sub>3</sub>); f) B. G. Hobrock and R. W. Kiser, *J. Phys. Chem.* **67**, 1283 (1963) (for CH<sub>3</sub>SSSCH<sub>3</sub>).
- [20] M. Suama and Y. Takezaki, *Bull. Inst. Chem. Res. Kyoto Univ.* **40**, 229 (1962).
- [21] D. L. Singleton, R. S. Irwin and R. J. Cvetanovic, *Can. J. Chem.* **61**, 968 (1983).
- [22] L. Bonazzola, A. H. Fuchs, J. Roncin, and H. Szwarc, *J. Phys. Chem.* **88**, 3003 (1984).
- [23] E. Block and J. O'Connor, *J. Am. Chem. Soc.* **96**, 3929 (1974).
- [24] D. M. Graham, R. L. Mievielle, R. H. Pallen, and C. Sivertz, *Can. J. Chem.* **42**, 2250 (1964).
- [25] M. N. Kogan, *Rarefied Gas Dynamics*, p. 458ff., Plenum Press, New York 1969.
- [26] J. B. Fenn and J. B. Anderson, in: *Advances in Applied Mechanics*, Suppl. 3: *Rarefied Gas Dynamics*, ed. J. H. de Leeuw, Vol. II, p. 311, Academic Press, New York 1966.
- [27] W. S. Nip, D. L. Singleton, and R. J. Cvetanovic, *J. Am. Chem. Soc.* **103**, 3526 (1981); R. J. Cvetanovic, D. L. Singleton, and R. S. Irwin, *J. Am. Chem. Soc.* **103**, 3530 (1981).